

State estimation of an electrochemical lithium-ion battery model: improved observer performance by hybrid redesign*

E. Petri¹, T. Reynaudo¹, R. Postoyan¹, D. Astolfi², D. Nešić³ and S. Raël⁴

Abstract—Effective management and just-in-time maintenance of lithium-ion batteries require the knowledge of unmeasured (internal) variables that need to be estimated. Observers are thus designed for this purpose using a mathematical model of the battery internal dynamics. It appears that it is often difficult to tune the observers to obtain good estimation performances both in terms of convergence speed and accuracy, while these are essential in practice. In this context, we demonstrate how a recently developed hybrid multi-observer can be used to improve the performance of a given observer designed for an electrochemical model of a lithium-ion battery. Simulation results, obtained with standard parameters values, show the estimation performance improvement using the proposed method.

I. INTRODUCTION

Lithium-ion batteries are widely used for the many advantages they exhibit in terms of volume capacity, weight, power density and the absence of memory effect, compared to other energy storage technologies. On the other hand, the so-called battery management system (BMS) is required for a safe and efficient usage of the battery. The BMS impacts the battery performance and lifespan and it depends on the actual state of charge (SOC) of the battery, which is directly related to the lithium concentrations in the battery electrodes. An accurate knowledge of the SOC is therefore essential for proper battery management. Unfortunately, the SOC cannot be measured directly and thus needs to be estimated from the measured variables, typically the current and the voltage. To address this challenge, a common approach is to design observers, based on a mathematical model of the internal dynamics, to estimate the unmeasured internal states, see e.g., [1], [2]. This task is non-trivial because of the nonlinear relationships between the internal variables and the measured ones. Several approaches are available in the literature depending on the type of battery model (equivalent circuit model, infinite/finite-dimensional electrochemical models) and the type of observers, see, e.g., [3]–[11].

In this work, we focus on the finite-dimensional electrochemical model considered in [9], [10], [12], which is

derived from the infinite-dimensional models in [6], [7], as it offers a good compromise between accuracy and computational complexity. The model takes the form of an affine system with a nonlinear output map, where the system states are the lithium concentrations in the electrodes, the input is the current and the measured output is the voltage. A globally convergent observer was designed for this model in [9] based on a polytopic approach. The issue is that to tune this observer to obtain both fast convergence and good robustness properties with respect to measurement noise and model uncertainties is highly non-trivial. The objective of this work is to address this challenge by systematically improving the estimation performance of an observer designed as in [9] using a multi-observer approach (see, e.g., [13, Section 8.3]). In particular, we follow the hybrid methodology we recently developed in [14], which consists in first designing a nominal observer using [9] that satisfies an input-to-state stability property. Then, a bank of additional observer-like systems, that differ from the nominal one only on their gains, are added in parallel to the nominal observer. The gains of these additional dynamical systems can be arbitrary selected and do not need to be tuned to guarantee a convergence property of their estimation errors. These gains can thus be selected using any analytical or heuristic method to improve the convergence speed or the robustness of the nominal observer. Each of these systems, as well as the nominal observer, is called mode for the sake of convenience. To evaluate the performance of each mode, monitoring variables are introduced. Based on these monitoring variables, the “best mode” is then selected at any time instant and its state estimate is considered for the battery internal state estimation. Therefore, the state estimate of the hybrid multi-observer switches between the states estimates of the modes and thus it is called hybrid. The observer is modeled as an hybrid system using the formalism of [15]. Note that, due to these switching, the state estimate exhibits discontinuities, which can be a problem for batteries, as this means the SOC estimate would experience jumps. For this reason, in this work, we add a filtered version of the hybrid multi-observer state estimate to the observer presented in [14]. We provide an input-to-state stability property with respect to measurement noise, perturbation and disturbance for the new hybrid system and, as in [14], we show that the performance of the hybrid multi-observer is, at least, as good as the performance of the nominal observer [9]. To illustrate the efficiency of the hybrid scheme, we present simulation results where a higher fidelity model of the battery is used to generate the output voltage compared to the one used to

*This work was funded by Lorraine Université d'Excellence LUE, HANDY project ANR-18-CE40-0010-02, the France Australia collaboration project IRP-ARS CNRS and the Australian Research Council under the Discovery Project DP200101303.

¹ E. Petri, T. Reynaudo and R. Postoyan are with the Université de Lorraine, CNRS, CRAN, F-54000 Nancy, France. (elena.petri@univ-lorraine.fr).

² D. Astolfi is with Université Claude Bernard Lyon 1, CNRS, LAGEPP UMR 5007, F-69100, Villeurbanne, France.

³ D. Nešić is with the Department of Electrical and Electronic Engineering, The University of Melbourne, Parkville, 3010 Victoria Australia.

⁴ S. Raël is with Université de Lorraine, GREEN, F-54000 Nancy, France.

design the observers. Using the technique in [9], we first design the nominal observer, which shows good transient performance in terms of speed and small overshoot, but whose accuracy in steady-state may not be satisfactory. To address this issue, we select the gains of the additional modes of the hybrid multi-observer [14] smaller than the nominal one, with the aim of improving the robustness to noises and perturbations. Simulation results show that the estimation performance are significantly improved with the hybrid multi-observer [14], thereby illustrating the potential of this approach.

Notation. The notation \mathbb{R} stands for the set of real numbers, $\mathbb{R}_{\geq 0} := [0, +\infty)$ and $\mathbb{R}_{> 0} := (0, +\infty)$. We use \mathbb{Z} to denote the set of integers, $\mathbb{Z}_{\geq 0} := \{0, 1, 2, \dots\}$ and $\mathbb{Z}_{> 0} := \{1, 2, \dots\}$. For a vector $x \in \mathbb{R}^n$, $\|x\|$ denotes its Euclidean norm. For a matrix $A \in \mathbb{R}^{n \times m}$, $\|A\|$ stands for its 2-induced norm. For a signal $v : \mathbb{R}_{\geq 0} \rightarrow \mathbb{R}^{n_v}$ with $n_v \in \mathbb{Z}_{> 0}$, and $t_1, t_2 \in \mathbb{R}_{\geq 0} \cup \{\infty\}$ with $t_1 \leq t_2$, $\|v\|_{[t_1, t_2]} := \text{ess sup}_{t \in [t_1, t_2]} |v(t)|$. Given a set $\mathcal{U} \subseteq \mathbb{R}^{n_u}$, $\mathcal{L}\mathcal{U}$ is the set of all functions from $\mathbb{R}_{\geq 0}$ to \mathcal{U} that are Lebesgue measurable and locally essentially bounded. Given a real, symmetric matrix P , its maximum and minimum eigenvalues are denoted by $\lambda_{\max}(P)$ and $\lambda_{\min}(P)$ respectively. The notation I_N stands for the identity matrix of dimension $N \in \mathbb{Z}_{> 0}$ and $0_{n \times m}$ stands for the null matrix of dimension $n \times m$, with $n, m \in \mathbb{Z}_{> 0}$. We consider \mathcal{K}_∞ and \mathcal{KL} functions, see [15, Definitions 3.4 and 3.38].

II. ELECTROCHEMICAL BATTERY MODEL

Before presenting the estimation scheme, we recall the single particle model of lithium-ion battery of [10].

The lithium-ion battery cell, whose schematic is shown in Fig. 1, is composed of four elements: two electrodes, one positive and one negative, that are separated by the separator and those three components are immersed in a ionic solution, called electrolyte, which can exchange lithium with the electrodes and provides electrical insulation. Therefore, the electrons cannot be exchanged from one electrode to the other. Due to the electrodes structure, which consists in very small, almost-spherical particles made of porous materials, the electrolyte can penetrate inside the electrode, creating a large contact surface between each electrode and the electrolyte, which produces an electrochemical coupling between the electrode material and the lithium dissolved in the electrolyte. Thus, each electrode has a certain potential and this produces a potential difference between the positive and negative electrode. Since the electrons cannot be exchanged from one electrode to the other within the battery, they will go through an external electrical circuit, if it exists, producing a flow of electrons, that from a macroscopic point of view, corresponds to the current. Note that the charges equilibrium in the electrodes and in the electrolyte is preserved at any time because when lithium is removed from its source electrode, another is inserted in its electrode of destination. The model in [10] relies on the next assumption.

Assumption 1. *The following hold: (i) the insertion/de-insertion reaction rate is homogeneous throughout the thickness of each electrode; (ii) the electrolyte dynamics is*

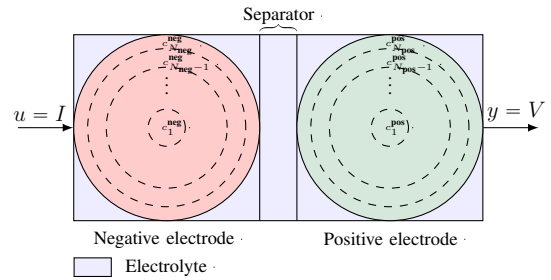


Fig. 1. Battery model schematic

neglected; (iii) the temperature is homogeneous and constant. \square

Item (i) implies that each electrode can be reduced to a single sphere particle of the average size of the particles that compose the actual electrode, which is the single particle model (SPM) as in [8]–[10], [16], [17]. In view of item (ii) of Assumption 1, the electrolyte contribution to the output voltage will be represented by a resistive term. However, we will relax this item in the simulation section to evaluate the estimation scheme robustness, see Section IV. On the other hand, it is possible to relax the constant temperature assumption in item (iii) of Assumption 1 in view of [10, Sections II.A and III.B], this is left for future work.

As explained in [10], in view of item (i) of Assumption 1, the main physical phenomenon is the lithium diffusion in the electrodes, which can be described using partial differential equations [6], [7]. To simplify the model and obtain a set of ordinary differential equations, each sphere is spatially discretized in N_s samples of uniform volume, corresponding to N_s crowns, where the subscript $s \in \{\text{neg}, \text{pos}\}$ denotes the negative or the positive electrode, see Fig. 1. We assume for this purpose that the lithium concentration in each crown of the sphere is constant. We denote by c_i^s , with $i \in \{1, \dots, N_s\}$ and $s \in \{\text{neg}, \text{pos}\}$, the lithium concentration in the i^{th} crown of the electrode, where $i = 1$ corresponds to the one at the center of the electrode, while $i = N_s$ corresponds to the one at the surface of the electrode. We also note that the lithium concentration at the center of the negative electrode c_1^{neg} can be expressed as a linear combination of all other sampled concentrations in solid phase by mass conservation, and consequently, it does not need to be a system state; see [10, Section II.C] for more details.

We consider the state-space model of the lithium-ion battery presented in [10], where the system state corresponds to the vector of the lithium concentrations in each sample of both electrodes $x := (c_2^{\text{neg}}, \dots, c_{N_{\text{neg}}}^{\text{neg}}, c_1^{\text{pos}}, \dots, c_{N_{\text{pos}}}^{\text{pos}}) \in \mathbb{R}^{n_x}$, with $n_x := N_{\text{neg}} + N_{\text{pos}} - 1$, the system input u is the current I and the system output y is the output voltage. The model is of the form

$$\begin{aligned} \dot{x} &= Ax + Bu + K + Ev \\ y &= h(x) + g(u) + w, \end{aligned} \quad (1)$$

The definitions of the matrices $A \in \mathbb{R}^{n_x \times n_x}$, $B \in \mathbb{R}^{n_x \times 1}$, $K \in \mathbb{R}^{n_x \times 1}$ and the function $g(u)$ for any $u \in \mathbb{R}$ are given in Appendix A. The function $h : \mathbb{R}^{n_x} \rightarrow \mathbb{R}$ is defined as, for any $x \in \mathbb{R}^{n_x}$, $h(x) := \text{OCV}_{\text{pos}}(H_{\text{pos}}x) - \text{OCV}_{\text{neg}}(H_{\text{neg}}x)$,

with $H_{\text{neg}} := (0_{1 \times (N_{\text{neg}}-2)}, \frac{1}{c_{\text{neg}}^{\text{max}}}, 0_{1 \times N_{\text{pos}}}) \in \mathbb{R}^{1 \times n_x}$, $H_{\text{pos}} := (0_{1 \times (N-1)}, \frac{1}{c_{\text{pos}}^{\text{max}}}) \in \mathbb{R}^{1 \times n_x}$ and the functions $\text{OCV}_s : \mathbb{R} \rightarrow \mathbb{R}$, with $s \in \{\text{neg}, \text{pos}\}$ are the open circuit voltages, which are the potential difference between the electrodes and the electrolyte without current and vary with the lithium concentration at the surface of the electrodes. An example of the OCVs is shown in Fig. 2. In (1), $E \in \mathbb{R}^{n_x \times n_v}$, $v \in \mathbb{R}^{n_v}$ is an unknown disturbance input and $w \in \mathbb{R}$ is an unknown exogenous input affecting the output map. We assume that $u : \mathbb{R}_{\geq 0} \rightarrow \mathbb{R}^{n_u}$, $v : \mathbb{R}_{\geq 0} \rightarrow \mathbb{R}^{n_v}$ and $w : \mathbb{R}_{\geq 0} \rightarrow \mathbb{R}$ are such that $u \in \mathcal{L}_{\mathcal{U}}$, $v \in \mathcal{L}_{\mathcal{V}}$ and $w \in \mathcal{L}_{\mathcal{W}}$ for closed sets $\mathcal{U} \subseteq \mathbb{R}^{n_u}$, $\mathcal{V} \subseteq \mathbb{R}^{n_v}$ and $\mathcal{W} \subseteq \mathbb{R}$, which is very reasonable for lithium-ion batteries.

The lithium concentrations in the electrodes are related to the state of charge (SOC) of the battery, which is an essential information. Indeed, the SOC is defined as, for all $t \geq 0$,

$$\text{SOC}(t) := 100 \frac{\bar{c}^{\text{pos}}(t) - c_0^{\text{pos}}}{c_{100}^{\text{pos}} - c_0^{\text{pos}}} \quad (2)$$

with $\bar{c}^{\text{pos}}(t) := \frac{1}{V_{\text{total}}^{\text{pos}}} \sum_{i=1}^{N_{\text{pos}}} c_i^{\text{pos}}(t) V_i^{\text{pos}}$, where c_0^{pos} and c_{100}^{pos} are the lithium concentrations in the positive electrode at SOC = 0 % and at SOC = 100 %, respectively, $V_{\text{total}}^{\text{pos}}$ is the total volume of the positive electrode and V_i^{pos} is the volume of the i^{th} sample of the positive electrode. The concentrations in the positive electrode are considered in (2); the same value for the SOC would be obtained by considering the concentrations in the negative electrode. Hence by estimating the concentrations in the electrodes, we will be able to also estimate the SOC. We now design an estimation scheme for this purpose.

III. HYBRID MULTI-OBSERVER DESIGN

The hybrid multi-observer consists of the following elements:

- *nominal observer*, here we consider the one proposed in [9], which satisfies an input-to-state stability property, as required by [14, Assumption 1];
- N additional dynamical systems with the same structure as the nominal observer, but with a different output injection gain, that can be arbitrarily selected. Each of these systems, as well as the nominal observer, is called *mode* for the sake of convenience;
- *monitoring variables* used to evaluate the performance of each mode of the multi-observer;
- *selection criterion*, that selects one mode of the multi-observer at any time instant, based on the performance knowledge given by the monitoring variables;
- *reset rule*, that updates the estimation scheme when a switching of the selected mode occurs;
- *filtered version* of the hybrid multi-observer state estimate to produce a continuous state estimate. Note that this is a novelty compared to [14].

A. Nominal observer

Inspired by [9], we design a nominal observer that satisfies the input-to-state stability property in [14, Assumption 1]. We make the next assumption for this purpose.

Assumption 2. *The parameters of the model are known.* \square

The nominal observer has the form

$$\begin{aligned} \dot{\hat{x}}_1 &= A\hat{x}_1 + Bu + K + L_1(y - \hat{y}_1) \\ \hat{y}_1 &= h(\hat{x}_1) + g(u), \end{aligned} \quad (3)$$

where $\hat{x}_1 \in \mathbb{R}^{n_x}$ is the state estimate, $\hat{y}_1 \in \mathbb{R}$ is the estimated output and $L_1 \in \mathbb{R}^{n_x \times 1}$ is the output injection gain, that needs to be designed; we use the subscript 1 because the nominal observer in (3) is the first element of the multi-observer that we will design in Section III-B. While (3) involves the plant input u , possible mismatches on the input current known by the plant and the observer, which often occur in practice, can be modeled using the disturbance input v and the exogenous input w in (1), as we will do in Section IV. We define the state estimation error as $e_1 := x - \hat{x}_1$. As in [14, Assumption 1], we define a perturbed version of the e_1 -dynamics, which is given by, in view of (1) and (3),

$$\dot{e}_1 = Ae_1 + Ev - L_1(h(x) - h(\hat{x}_1)) - L_1w + d, \quad (4)$$

where $d \in \mathbb{R}^{n_x}$ represents an additional artificial perturbation on the output injection term $L_1(y - \hat{y}_1)$. To consider the perturbed dynamics in (4) with extra input d is required to check one of the key assumptions of [14], which is needed to establish the main result of the work.

We design the observer gain L_1 to guarantee a convergence property of the estimation error e_1 . In particular, L_1 has to be designed such that the origin of (4) satisfies an input-to-state stability property with respect to v , w and d . To design the observer gain L_1 , we make the next assumption on the OCVs, which is taken from [9, Assumption 5].

Assumption 3. *There exist constant matrices $C_1, \dots, C_4 \in \mathbb{R}^{1 \times n_x}$ such that, for any $x, x' \in \mathbb{R}^{n_x}$,*

$$h(x) - h(x') = C(x, x')(x - x'), \quad (5)$$

where $C(x, x') := \sum_{i=1}^4 \lambda_i(x, x') C_i$, with $\lambda_i \in [0, 1]$, $\sum_{i=1}^4 \lambda_i(x, x') = 1$ and $i \in \{1, \dots, 4\}$. \square

Assumption 3 means that the output map h lies in a polytope defined by the vertices C_i , with $i \in \{1, \dots, 4\}$. This condition is often verified in practice. Indeed, the OCVs are generally defined on the interval $[0, 1]$ by experimental data and they are well-approximated by a piecewise continuously differentiable function. Moreover, the OCVs only depend on the surface lithium concentration of the negative and positive electrode. Consequently, the output map h only depends on two states of the system and the set of C_i has only 2^2 elements, which are obtained from the maximum and minimum slopes of the OCVs. Using Assumption 3, (4) becomes

$$\dot{e}_1 = (A - L_1 C(x, \hat{x}_1))e + Ev - L_1w - d. \quad (6)$$

To design the observer output injection gain L_1 we follow a polytopic approach and we propose a modified version of [9, Theorem 1] below.

Theorem 1. Consider system (6). If there exist $L_1 \in \mathbb{R}^{n_x \times 1}$, α, μ_v, μ_w and $\mu_d \in \mathbb{R}_{>0}$ and $P \in \mathbb{R}^{n_x \times n_x}$ symmetric positive definite such that

$$\begin{pmatrix} \mathcal{H}_i + \alpha P & PE & -PL_1 & -P \\ E^\top P & -\mu_v I_{n_v} & 0 & 0 \\ -L_1^\top P & 0 & -\mu_w I_{n_w} & 0 \\ -P & 0 & 0 & -\mu_d I_{n_x} \end{pmatrix} \leq 0, \quad (7)$$

with $\mathcal{H}_i := (A - L_1 C_i)^\top P + P(A - L_1 C_i)$ for all $i \in \{1, \dots, 4\}$. Then $V : e_1 \mapsto e_1^\top P e_1$ satisfies, for any $e_1 \in \mathbb{R}^{n_x}$, $v \in \mathcal{V}$, $w \in \mathcal{W}$ and $d \in \mathbb{R}^{n_x}$,

$$\lambda_{\min}(P)|e_1|^2 \leq V(e_1) \leq \lambda_{\max}(P)|e_1|^2, \quad (8)$$

$$\begin{aligned} \langle \nabla V(e_1), (A - L_1 C(x, \hat{x}_1))e_1 - L_1 w \rangle \\ \leq -\alpha V(e_1) + \mu_v |v|^2 + \mu_w |w|^2 + \mu_d |d|^2. \end{aligned} \quad (9)$$

□

The proof of Theorem 1 follows similar steps as [9, proof of Theorem 1] and is therefore omitted. Theorem 1 guarantees that the nominal observer (3) satisfies an input-to-state stability property with respect to the disturbance v , the exogenous perturbation w and the additional perturbation d . This implies that the estimation error e_1 exponentially converges to a neighborhood of the origin, whose “size” depends on the \mathcal{L}_∞ norm of v , w and d . As a result, [14, Assumption 1] is satisfied. The possible drawback of observer (3) with L_1 designed as in Theorem 1 is that to tune the observer gain L_1 to obtain good estimation performance both in speed of convergence and robustness to measurement noise, exogenous perturbation and disturbance is very difficult in general. For this reason, we apply our recent result in [14], which consists in designing a hybrid multi-observer with the aim of improving the estimation performance of (3).

B. Hybrid multi-observer

To improve the estimation performance of the nominal observer (3), we design the hybrid multi-observer proposed in [14]. For this purpose, we consider N additional dynamical systems with the form of (3), where the number $N \in \mathbb{Z}_{>0}$ is freely selected by the user, but with a different output injection gain, i.e., for any $k \in \{2, \dots, N+1\}$, the k^{th} mode of the multi-observer is given by

$$\begin{aligned} \dot{\hat{x}}_k &= A\hat{x}_k + Bu + K + L_k(y - \hat{y}_k) \\ \hat{y}_k &= h(\hat{x}_k) + g(u), \end{aligned} \quad (10)$$

where $\hat{x}_k \in \mathbb{R}^{n_x}$ is the mode k state estimate, $\hat{y}_k \in \mathbb{R}$ is the mode k estimated output and $L_k \in \mathbb{R}^{n_x \times 1}$ is its output injection gain. Since there is full freedom on the selection of the gains L_k , with $k \in \{2, \dots, N+1\}$, there are no convergence guarantees on the estimation errors $e_k := x - \hat{x}_k$, with $k \in \{2, \dots, N+1\}$. A recommended approach to select the gains L_k 's is to consider the behaviour of the nominal observer in (3) in simulation and, based on that, to select the additional gains depending on the property we want to improve. For instance, if the convergence speed of the estimation error e_1 is too slow, we may define the L_k by increasing the values of L_1 . On the opposite, if the

convergence speed of e_1 is satisfactory but its accuracy for large time is not satisfactory, we may select the gains L_k with small values, as we will do in Section IV. There are many other approaches that can be followed to select the additional gains. For example, we may pick them in a neighborhood of the nominal one or design one additional gain for each vertex of the polytope. Note that these gain selection criteria may result in diverging estimation errors for some of the modes, still the overall hybrid scheme we present does ensure the (approximate) convergence of the obtained state estimation error to the origin.

To select which state estimate \hat{x}_k , $k \in \{1, \dots, N+1\}$, we need to consider, we evaluate which mode has the best performance. To define performance, we introduce monitoring variables, denoted $\eta_k \in \mathbb{R}_{\geq 0}$, with $k \in \{1, \dots, N+1\}$, whose dynamics are

$$\dot{\eta}_k = -\nu \eta_k + \lambda_1 |y - \hat{y}_k|^2 + \lambda_2 |L_k(y - \hat{y}_k)|^2, \quad (11)$$

where $\lambda_1, \lambda_2 \in \mathbb{R}_{\geq 0}$, with $\max(\lambda_1, \lambda_2) > 0$ and $\nu \in (0, \alpha]$, are design parameters, with α from Theorem 1. The condition $\nu \in (0, \alpha]$ is required to establish the stability property formalized in [14]. The monitoring variable dynamics is inspired by [18] and depends both on output estimation error, with the term $\lambda_1 |y - \hat{y}_k|^2$, and on the correction effort of the observer, with $\lambda_2 |L_k(y - \hat{y}_k)|^2$. This last term is called latency in [18]. Equation (11) implies that, for any $k \in \{1, \dots, N+1\}$, for any initial condition $\eta_k(0) \in \mathbb{R}_{\geq 0}$, for any $y, \hat{y}_k \in \mathcal{L}_{\mathbb{R}^{n_y}}$ and any $t \geq 0$,

$$\begin{aligned} \eta_k(t) &= e^{-\nu t} \eta_k(0) + \int_0^t e^{-\nu(t-\tau)} (\lambda_1 |y(\tau) - \hat{y}_k(\tau)|^2 \\ &\quad + \lambda_2 |L_k(y(\tau) - \hat{y}_k(\tau))|^2) d\tau. \end{aligned} \quad (12)$$

From (12) we have that the monitoring variables represent the cost of the modes. Consequently, the idea is to select the mode that produces the minimum monitoring variable, and thus the minimum cost, at any time instant. Note that, we can freely choose the initial conditions of these monitoring variables, $\eta_k(0) \in \mathbb{R}_{\geq 0}$, with $k \in \{1, \dots, N+1\}$. This extra degree of freedom can be used to initially select or penalize one or more modes of the multi-observer, as we do in simulation in Section IV. The signal $\sigma : \mathbb{R}_{\geq 0} \rightarrow \{1, \dots, N+1\}$ is used to indicate the selected mode at any time instant. The corresponding state estimate, monitoring variable and state estimation error are denoted \hat{x}_σ , η_σ and e_σ , respectively. We denote with $t_0 = 0$ the initial time and with $t_i \in \mathbb{R}_{\geq 0}$, $i \in \mathbb{Z}_{>0}$ the times when a switch of the selected mode occurs, i.e., $t_i := \inf\{t \geq t_{i-1} : \exists k \in \{1, \dots, N+1\} \setminus \{\sigma(t)\} \text{ such that } \eta_k(t) \leq \varepsilon \eta_\sigma(t)\}$, where $\varepsilon \in (0, 1]$ is a design parameter introduced to mitigate the occurrence of fast switching. Consequently, for all $i \in \mathbb{Z}_{>0}$, $\dot{\sigma}(t) = 0$ for all $t \in (t_{i-1}, t_i)$ and $\sigma(t_i) \in \underset{k \in \{1, \dots, N+1\}}{\arg \min} \eta_k(t_i)$.

Finally, when switching occur, not only the signal σ is updated, but also the state estimates and the monitoring variables of the additional modes are reset to the ones of

the selected mode, ¹, i.e., at a switching time $t_i \in \mathbb{R}_{\geq 0}$, $i \in \mathbb{Z}_{>0}$,

$$\hat{x}_k(t_i^+) \in \{\hat{x}_{k^*}(t_i) : k^* \in \arg \min_{j \in \{1, \dots, N+1\}} \eta_j(t_i)\}, \quad (13)$$

$$\eta_k(t_i^+) \in \{\eta_{k^*}(t_i) : k^* \in \arg \min_{j \in \{1, \dots, N+1\}} \eta_j(t_i)\}, \quad (14)$$

where t_i^+ represent the time immediately after the switching instant t_i and $k \in \{2, \dots, N+1\}$.

The state estimate \hat{x}_σ produced by the hybrid multi-observer may be discontinuous. For this reason, we add a filtered version of \hat{x}_σ , denoted \hat{x}_f , whose dynamics between switching is given by

$$\dot{\hat{x}}_f = -\zeta \hat{x}_f + \zeta \hat{x}_\sigma, \quad (15)$$

where $\zeta > 0$ is an additional design parameter and, at switching times $t_i \in \mathbb{R}_{>0}$, with $i \in \mathbb{Z}_{>0}$,

$$\hat{x}_f(t_i^+) = \hat{x}_f(t_i). \quad (16)$$

C. Hybrid model and stability guarantees

Including \hat{x}_f , we obtain a new hybrid model for the hybrid multi-observer compared to [14], whose state is defined as $q := (x, \hat{x}_1, \dots, \hat{x}_{N+1}, \eta_1, \dots, \eta_{N+1}, \sigma, \hat{x}_f) \in \mathcal{Q} := \mathbb{R}^{n_x} \times \mathbb{R}^{(N+1)n_x} \times \mathbb{R}_{\geq 0}^{N+1} \times \{1, \dots, N+1\} \times \mathbb{R}^{n_x}$. The hybrid system is given by

$$\begin{cases} \dot{q} = F(q, u, v, w), & q \in \mathcal{C} \\ q^+ \in G(q), & q \in \mathcal{D}, \end{cases} \quad (17)$$

where the flow map F is obtained from (1), (3), (10), (11) and (15), the jump map G follows from the above developments, (16) and is similar to the jump map in [14]. The flow and jump sets, \mathcal{C} and \mathcal{D} , are defined as

$$\mathcal{C} := \{q \in \mathcal{Q} : \forall k \in \{1, \dots, N+1\} \quad \eta_k \geq \varepsilon \eta_\sigma\}, \quad (18)$$

$$\mathcal{D} := \{q \in \mathcal{Q} : \exists k \in \{1, \dots, N+1\} \setminus \{\sigma\} \quad \eta_k \leq \varepsilon \eta_\sigma\}. \quad (19)$$

The next theorem ensures that system (17) satisfies a two-measure input-to-state stability property with respect to the disturbance v and the perturbation w [19].

Theorem 2. *Consider system (17) and suppose Assumptions 1-3 hold and L_1 is selected such that condition (7) in Theorem 1 is satisfied. Then, there exist $\beta_U \in \mathcal{KL}$ and $\gamma_U \in \mathcal{K}_\infty$ such that for any input $u \in \mathcal{L}_U$, disturbance input $v \in \mathcal{L}_V$ and exogenous perturbation $w \in \mathcal{L}_W$, any solution q satisfies*

$$\begin{aligned} & |(e_1(t, j), \eta_1(t, j), e_\sigma(t, j), \eta_\sigma(t, j), e_f(t, j))| \\ & \leq \beta_U(|(e(0, 0), \eta(0, 0))|, t) + \gamma_U(\|v\|_{[0, t]} + \|w\|_{[0, t]}) \end{aligned} \quad (20)$$

for all (t, j) in the domain² of the solution q , with $e := (e_1, \dots, e_{N+1})$, $\eta := (\eta_1, \dots, \eta_{N+1})$, $e_\sigma := x - \hat{x}_\sigma$ and $e_f := x - \hat{x}_f$. \square

¹In [14] two possible reset rules are considered, called without and with resets. Only the reset strategy is considered in this work.

²The solution q of the hybrid multi-observer is defined on hybrid-time domains, see [15, Definition 2.3], where the first argument is the continuous time t , while the second argument is the discrete time j and represents the number of jumps/switching.

Sketch of proof: We first note that all the conditions of [14, Theorem 1] are satisfied. Indeed, thanks to Theorem 1, [14, Assumption 1] holds. Moreover, [14, Assumption 2] is satisfied thanks to Assumption 3 and because the Lyapunov function V in Theorem 1 is quadratic. We can then follow similar steps as in [14, proofs of Proposition 1 and Theorem 1] to obtain the desired result. Note that, having \hat{x}_f as part of the hybrid state is not a problem. Indeed, it does not change at jumps from (16) and, from (15), it is an input-to-state stable system in cascade with the hybrid system used in [14, Theorem 1], see [20, Section 4]. \blacksquare

Theorem 2 ensures that the estimation errors and the monitoring variables of the nominal observer e_1 and η_1 converge to a neighborhood of the origin, whose “size” depends on the \mathcal{L}_∞ norm of v and w , which is not surprising in view of Theorem 1. However, Theorem 2 also guarantees that the state estimation error and the monitoring variable of the hybrid multi-observer e_σ and η_σ and also the filtered version of the estimation error, namely e_f , converge to the same neighborhood of the origin. Hence, the convergence of the (filtered) state estimate produced by the hybrid scheme is guaranteed despite the fact that the gains L_k in (10) were freely selected. Moreover, when $\varepsilon = 1$, we have that $\eta_{\sigma(t, j)}(t, j) \leq \eta_1(t, j)$, for all (t, j) in the domain of the solution q . Therefore, the estimation performance of the hybrid multi-observer are always not worse than the nominal one, according to the considered performance cost. We will see in the next section that significant performance improvements can be obtained in simulations.

IV. NUMERICAL STUDY

In this section, we compare the estimates generated by a nominal observer (3) and the associated hybrid multi-observer (17) with standard parameter values.

A. System model

We assume that each electrode is composed of 6 samples with identical volumes. Consequently, $N_{\text{neg}} = N_{\text{pos}} = 6$ and $n_x = N_{\text{neg}} - 1 + N_{\text{pos}} = 11$. We consider the parameters in Table II in the appendix. We take a measurement noise equal to $0.05 \sin(30t)$ V, which has a reasonable frequency and signal versus noise ratio for embedded battery voltage measurements. The input w in (1) is given by $w = 0.05 \sin(30t) + w_2(t)$ where w_2 is an additional term due to the input mismatch between the battery and its observer as clarified in the sequel. The considered OCV curves for the positive and the negative electrodes are shown in Fig. 2, which satisfy Assumption 3 and [14, Assumption 2].

B. Input current

The input u is given by a Plug-in Hybrid Electrical Vehicles (PHEV) current profile [21]. In practical applications, the observer usually only knows a biased version of the battery current. This bias is due to the precision of the sensor and its conditioning. We therefore introduce I_{biased} to denote the input u known by the observer, which is given by $I_{\text{biased}}(t) = 0$ when $I(t) = 0$, $I_{\text{biased}}(t) =$

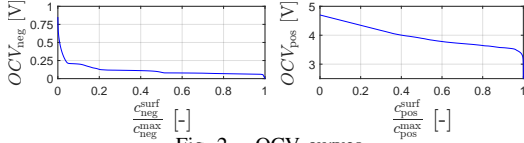


Fig. 2. OCV curves

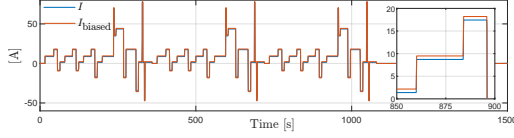


Fig. 3. Input current profile and its biased version available to the observer

$I(t) + 0.01 \max_{t^* \in [0, t]} |I(t^*)|$ when $I(t) > 0$ and $I_{\text{biased}}(t) = I(t) - 0.01 \max_{t^* \in [0, t]} |I(t^*)|$ when $I(t) < 0$, for all $t \geq 0$. We

consider a precision of 1% on the full scale for the current bias, which corresponds to a standard sensor. The PHEV current input I and its biased version I_{biased} are shown in Fig. 3. This mismatch in the current input of system and observer can be modeled using the disturbance input v and the exogenous perturbation w in (1). Indeed, the plant input $u = I = I_{\text{biased}} + v$, where v is defined as $v := I - I_{\text{biased}}$. With the matrix E equal to the matrix B , we obtain $\dot{x} = Ax + BI_{\text{biased}} + K + Bv$. Moreover, to model the input mismatch in the output map, we define $w_2 = g(I_{\text{biased}}) - g(I)$, so that w in (1) is $w = 0.05 \sin(30t) + g(I_{\text{biased}}) - g(I)$.

C. Electrolyte dynamics

To test the robustness of the estimation scheme, we consider a model of the electrolyte dynamics, as in [11, Section IV.B], thereby relaxing item (ii) in Assumption 1. Consequently, the battery output voltage becomes

$$y = \varrho_{\text{pos}} - \varrho_{\text{neg}} - \varrho_{\text{sep}}, \quad (21)$$

where y is the battery output from (1) and ϱ_r , with $r \in \{\text{pos}, \text{neg}, \text{sep}\}$, is the electrolyte diffusional overvoltage in the positive electrode, negative electrode or separator, which dynamics is given by $\dot{\varrho}_r = -\varrho_r/\varsigma_{1,r} + u\varsigma_{2,r}/\varsigma_{1,r}$, where $\varsigma_{1,r}$ and $\varsigma_{2,r}$ are the ionic diffusion time constant and ionic diffusion resistance in r . However, these electrolyte dynamics are ignored below when designing the nominal observer and the additional modes.

D. Nominal observer

We now design the nominal observer in (3). To test its efficiency, we design it with a smaller number of samples compared to the system model in (1). In this way, a higher fidelity model is used to generate the output voltage. We thus select $N_{\text{neg, obs}} = N_{\text{pos, obs}} = 4$ and $n_{x, \text{obs}} = N_{\text{neg, obs}} - 1 + N_{\text{pos, obs}} = 7$, while the battery model is $11 + 3$, where the 3 additional dimensions are due to the electrolyte dynamics in Section IV-C. We then solve (7) and we obtain $L_1 = (28.03, 27.78, 28.77, -45.54, -45.72, -44.78, -46.28)$. The system is initialized with a state of charge of 100%, which corresponds to $x(0, 0) = (11.75, 11.75, 11.75, 11.75, 11.75, 9.182, 9.182, 9.182, 9.182,$

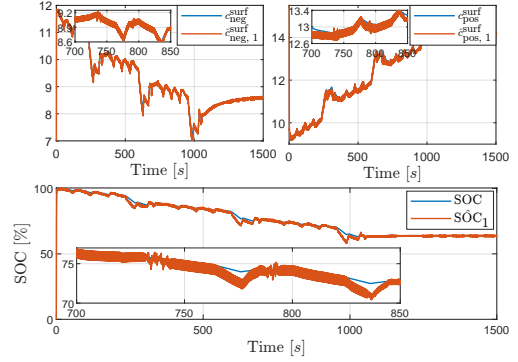


Fig. 4. Lithium concentrations at the surface of both electrodes $c_{\text{neg}}^{\text{surf}}$ (top figure left) and $c_{\text{pos}}^{\text{surf}}$ (top figure right), state of charge (SOC) (bottom figure). Reference system (blue), nominal observer (red).

9.182, 9.182), while the nominal observer is initialized with a state of charge of 0%, which corresponds to $\hat{x}_1(0, 0) = (3.069, 3.069, 3.069, 23.01, 23.01, 23.01, 23.01)$. Therefore, the state of charge estimation error is initialized at 100 %, which is the largest possible initial estimation error. The electrolytes diffusional overvoltages are initialized at $\varrho_r(0, 0) = 0$ for any $r \in \{\text{pos}, \text{neg}, \text{sep}\}$. The lithium surface concentrations, and their estimations, of both the negative and positive electrodes are shown in Fig. 4, together with the state of charge and its estimate.

The nominal observer has good performance in terms of speed of convergence, see Fig. 4. Indeed, despite the large initial error for the SOC, the nominal observer estimate converges fast to the actual SOC. However, the observer estimates is very sensitive to measurement noise, model mismatch and input bias, which impact the estimation performance especially when the estimation error reaches a neighborhood of the origin. Consequently, the hybrid multi-observer is designed in the next section with the aim of improving the estimation performance in terms of robustness to measurement noise, model mismatch and input bias, while preserving the fast convergence of the nominal observer.

E. Hybrid multi-observer

We design the multi-observer adding $N = 3$ additional modes (10) in parallel to the nominal observer. Since small gains typically help with respect to noise, we chose the additional gains smaller than the nominal one, even though they may not result in converging estimation errors. In particular, we select $L_2 = L_1/10$, $L_3 = L_1/100$ and $L_4 = 0_{7 \times 1}$. The gain $L_4 = 0_{7 \times 1}$ does not lead to a “converging mode” but it is the best choice to annihilate the measurement noise. Simulations suggest that the SOC estimation error of the modes with L_2 and L_3 converge, while the one with L_4 does not. Note that, in the choice of the additional gains we exploited the complete freedom given in Section III.

F. Initialization and design parameters

The state estimate of the additional modes, \hat{x}_k , with $k \in \{2, \dots, 4\}$ are initialized at the same value as \hat{x}_1 in Section IV-D. We select $\eta_1(0, 0) = 1$ and $\eta_k(0, 0) = 10$ for all $k \in \{2, 3, 4\}$, $\sigma(0, 0) = 1$ and $\hat{x}_f(0, 0) = \hat{x}_{\sigma(0, 0)}(0, 0) =$

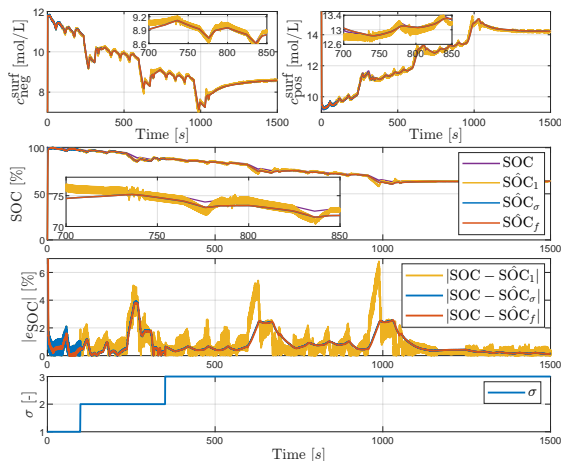


Fig. 5. Lithium concentrations at the surface of both electrodes $c_{\text{neg}}^{\text{surf}}$ (top figure left) and $c_{\text{pos}}^{\text{surf}}$ (top figure right), state of charge (SOC) (second figure), norm of the state of charge estimation error (third figure) and σ (bottom figure). Real system (purple), nominal (yellow), σ -estimate (blue), filtered estimate (red).

$\hat{x}_1(0, 0)$. This choice of initializing the nominal monitoring variable η_1 smaller than the monitoring variables of all the additional modes is because the transitory performance of the nominal observer is good and this choice, together with the initialization of σ at the nominal observer, allows to select the nominal observer for some amount of time at the beginning of the simulation. We simulate the proposed hybrid multi-observer with $\nu = 0.005$, $\lambda_1 = 1$, $\lambda_2 = 0.005$, $\varepsilon = 0.95$ and $\zeta = 3$. Note that, the condition $\nu \in (0, \alpha)$ in [14, Proposition 1] is satisfied. Indeed, for the considered lithium-ion battery, we have $\alpha = 0.01$ in Theorem 1.

G. Results

The lithium surface concentrations of both the negative and positive electrodes, namely $c_{\text{neg}}^{\text{surf}}$ and $c_{\text{pos}}^{\text{surf}}$, together with their estimates using the nominal observer, the hybrid multi-observer and its filtered version are shown in Fig. 5. We recall that the lithium surface concentrations are elements of the system state and therefore Fig. 5 shows that the hybrid multi-observer improve the state estimation performance compared to the nominal observer. Moreover, using (2), we obtain the state of charge (SOC) and its estimates with the nominal observer and the hybrid multi-observer (filtered and not) and, from these, we evaluate the norm of the state of charge estimation errors. The results are shown in Fig. 5, where we see that the state of charge estimate is improved, both on the averaged value and on the oscillations, using the hybrid multi-observer. The obtained performance improvement is commonly considered to be significant for this application. The last plot in Fig. 5 represents the signal σ which indicates the mode that is selected at every time instant.

To further evaluate the effectiveness of the proposed hybrid multi-observer, we have run 100 simulations with different initial conditions. In particular, the initial state of charge estimate of all the modes of the multi-observer $\hat{\text{SOC}}_k(0, 0)$, with $k \in \{1, \dots, 4\}$, were selected randomly in the interval $[0, 100]\%$, while the battery state of charge

TABLE I

AVERAGE MAE AND RMSE OF THE SOC ESTIMATION ERROR (e_{SOC}) FOR $t \in [0, 1500]$ s (TOT), $t \in [0, 150]$ s (TRAN) AND $t \in [150, 1500]$ s (END).

	$e_{\text{SOC},1}$	$e_{\text{SOC},\sigma}$	$e_{\text{SOC},f}$
MAE _{tot} [%]	0.82	0.76	0.76
MAE _{tran} [%]	0.83	0.81	0.84
MAE _{end} [%]	0.82	0.76	0.75
RMSE _{tot} [%]	1.65	1.47	1.64
RMSE _{tran} [%]	3.07	3.06	3.74
RMSE _{end} [%]	1.29	1.04	1.02

was always initialized at $\text{SOC}(0, 0) = 100\%$. We considered the same choice as before for all the design parameters and initial conditions of the monitoring variables η_k , with $k \in \{1, \dots, 4\}$, σ and ϱ_r , with $r \in \{\text{pos}, \text{neg}, \text{sep}\}$. To quantify the improvement brought by the hybrid multi-observer, we evaluate the mean absolute error (MAE) and the root mean square error (RMSE), averaged over all the simulations, on the SOC estimation error obtained with the nominal observer and the proposed hybrid multi-observer, filtered and not. The data collected are shown in Table I for the whole simulation time $t \in [0, 1500]$ s, during the transitory for $t \in [0, 150]$ s and after the transitory for $t \in [150, 1500]$ s.

Table I shows that the hybrid multi-observer unfiltered improves the estimation performance, especially at large times as desired. Indeed, both the MAE and the RMSE are always smaller compared to the ones of the nominal observer. Moreover, the filtered version, even if during transient has worse performance compared to the nominal observer, after the transient the improvement is clear and, the performance can be also better than the corresponding unfiltered version.

V. CONCLUSIONS

We have applied and extended the hybrid multi-observer proposed in [14] to improve the estimation performance of the observer based on a polytopic approach designed in [9] to estimate the lithium concentration of the electrodes of an electrochemical battery, which is directly related to the state of charge. Simulations based on standard model parameter values have illustrated the potential of this approach to improve the state of charge estimation performance.

In future work, we plan to include uncertainties in the design parameters and apply the proposed approach to experimental data.

APPENDIX

A. Model description

The matrices and function definitions in (1) are defined as

$$A := \begin{pmatrix} A_{2,\text{neg}} & \\ A^* & \text{diag}(A_{\text{neg}}, A_{\text{pos}}) \end{pmatrix}, \text{ with } A^* := \begin{pmatrix} \mu_{3,2}^{\text{neg}} \\ 0_{(n_x-2) \times 1} \end{pmatrix}, \quad (22)$$

where $A_{2,\text{neg}} \in \mathbb{R}^{1 \times n_x}$ is defined as

$$A_{2,\text{neg}} := \left(\tilde{\nu}_2^{\text{neg}}, \tilde{\nu}_2^{\text{neg}}, \nu_{2,1,4}^{\text{neg,neg}}, \dots, \nu_{2,1,N_{\text{neg}}}^{\text{neg,neg}}, \nu_{2,1,1}^{\text{neg,pos}}, \dots, \nu_{2,1,N_{\text{pos}}}^{\text{neg,pos}} \right),$$

TABLE II

PHYSICAL PARAMETERS OF THE ELECTROCHEMICAL MODEL

A_{cell}	Cell area [m^2]	1.0452
F	Faraday's constant [C/mol]	96485
R	Gas constant [$J/K/mol$]	8.3145
T	Temperature [K]	298.15
N	Order of the model [-]	7
d_{pos}	Thickness of the positive electrode [μm]	36
d_{neg}	Thickness of the negative electrode [μm]	50
D_{pos}	Lithium diffusion coefficient [m^2/s]	3.723×10^{-16}
D_{neg}	Lithium diffusion coefficient e [m^2/s]	2×10^{-16}
$c_{0,\text{pos}}$	Lithium concentration at SOC = 0% [$mol.L^{-1}$]	23.01
$c_{0,\text{neg}}$	Lithium concentration at SOC = 0% [$mol.L^{-1}$]	3.167
$c_{100,\text{pos}}$	Lithium concentration at SOC = 100% [$mol.L^{-1}$]	9.182
$c_{100,\text{neg}}$	Lithium concentration at SOC = 100% [$mol.L^{-1}$]	11.75
$c_{\text{max},\text{pos}}$	Maximum concentration [$mol.L^{-1}$]	23.9
$c_{\text{max},\text{neg}}$	Maximum concentration [$mol.L^{-1}$]	16.1
σ_{pos}	Electronic conductivity [S/m]	10
σ_{neg}	Electronic conductivity [S/m]	100
R_{pos}	Particle radius [μm]	1
R_{neg}	Particle radius [μm]	1
$j_{0,\text{pos}}$	Exchange current density [A/m^2]	0.5417
$j_{0,\text{neg}}$	Exchange current density [A/m^2]	0.75
ε_{pos}	Volume fraction of the material within the positive electrode [-]	0.5
ε_{neg}	Volume fraction of the material within the negative electrode [-]	0.58
Q_{Li}	Lithium quantity in cell solid phases [Ah]	14.8318
Q_{cell}	Cell capacity [Ah]	6.9725
Ω_{add}	Additional resistivity [Ω]	0
$\varsigma_{1,\text{pos}}$	Ionic diffusion time constant [s]	13.0
$\varsigma_{1,\text{neg}}$	Ionic diffusion time constant [s]	17.3
$\varsigma_{1,\text{sep}}$	Ionic diffusion time constant of separator [s]	12.3
$\varsigma_{2,\text{pos}}$	Ionic diffusion resistance [$\mu\Omega$]	153.9
$\varsigma_{2,\text{neg}}$	Ionic diffusion resistance [$\mu\Omega$]	209.5
$\varsigma_{2,\text{sep}}$	Ionic diffusion resistance of separator [$\mu\Omega$]	115.1

while $A_{\text{neg}} \in \mathbb{R}^{N_{\text{neg}}-2 \times N_{\text{neg}}-2}$, resp. $A_{\text{pos}} \in \mathbb{R}^{N_{\text{pos}} \times N_{\text{pos}}}$, as $A_{\text{neg}} := \text{diag}(\mu_{i,i-1}^{\text{neg}}) + \text{diag}(\tilde{\mu}_i^{\text{neg}}) + \text{diag}(\mu_{i,i}^{\text{neg}})$, $A_{\text{pos}} := \text{diag}(\mu_{i,i-1}^{\text{pos}}) + \text{diag}(\tilde{\mu}_i^{\text{pos}}) + \text{diag}(\mu_{i,i}^{\text{pos}})$, for $i \in \{3, \dots, N_{\text{neg}}\}$, resp., for $i \in \{1, \dots, N_{\text{pos}}\}$, where diag denotes the lower diagonal, $\overline{\text{diag}}$ denotes the upper diagonal, $\tilde{\nu}_2^{\text{neg}} := \nu_{2,1,2}^{\text{neg, neg}} - \mu_{2,1}^{\text{neg}} - \mu_{2,2}^{\text{neg}}$, $\tilde{\nu}_2^{\text{neg}} := \nu_{2,1,3}^{\text{neg, neg}} + \mu_{2,2}^{\text{neg}}$, $\mu_{i,j}^s := \frac{D_s}{V_i^s} \frac{S_j^s}{r_{j+1} - r_j}$, $\tilde{\mu}_i^s := -\mu_{i,i-1}^s - \mu_{i,i}^s$, $\nu_{i,j,z}^{s,s'} := \mu_{i,j}^s \beta_z^{s'}$, $\beta_i^{\text{neg}} := -\frac{V_i^{\text{neg}}}{V_1^{\text{neg}}}$, $\beta_i^{\text{pos}} := -\frac{\alpha_{\text{pos}} V_i^{\text{pos}}}{\alpha_{\text{neg}} V_1^{\text{neg}}}$, $\alpha_s := \frac{F}{3600} \frac{\varepsilon_s A_{\text{cell}} d_s}{V_{\text{tot}}^s}$, $D_s, V_i^s, S_i^s, r_i, \varepsilon_s, F, A_{\text{cell}}$ and d_s are defined in Table II, for any $i, j, z \in \{1, \dots, N_s\}$, $s, s' \in \{\text{neg}, \text{pos}\}$. The matrix B is defined as $B := (0_{(N_{\text{neg}}-2) \times 1} - \bar{K}_I^{\text{neg}} 0_{(N_{\text{pos}}-1) \times 1} \bar{K}_I^{\text{pos}})^{\top}$, with $\bar{K}_I^s := -\frac{S_{\text{tot}}^s}{V_1^s a_s F A_{\text{cell}} d_s}$, where $a_s := 3\varepsilon_s/R_s$, R_s is the radius and $s \in \{\text{neg}, \text{pos}\}$. The matrix K is defined as $K := (-\mu_{2,1}^{\text{neg}} \bar{K} 0_{(N-1) \times 1})^{\top}$, with $\bar{K} := \frac{Q_{\text{Li}}}{V_1^{\text{neg}} \alpha_{\text{neg}}}$, where Q_{Li} is the quantity of lithium in the solid phase. Finally, $g(u) := g_1(u) + g_2(u) + g_3(u)$, with $g_1(u) := 2 \frac{RT}{F} \text{Argsh}\left(\frac{-R_{\text{pos}}}{6\varepsilon_{\text{pos}} j_0^{\text{pos}} A_{\text{cell}} d_{\text{pos}}} u\right)$, $g_2(u) := -2 \frac{RT}{F} \text{Argsh}\left(\frac{R_{\text{neg}}}{6\varepsilon_{\text{neg}} j_0^{\text{neg}} A_{\text{cell}} d_{\text{neg}}} u\right)$, $g_3(u) := -\left(\frac{1}{2A_{\text{cell}}} \left(\frac{d_{\text{neg}}}{\sigma_{\text{neg}}} + \frac{d_{\text{pos}}}{\sigma_{\text{pos}}}\right) + \Omega_{\text{add}}\right) u$, where $\text{Argsh}(\xi) = \ln(\xi + \sqrt{\xi^2 + 1})$ for any $\xi \in \mathbb{R}$.

REFERENCES

- [1] H. He, R. Xiong, H. Guo, and S. Li, "Comparison study on the battery models used for the energy management of batteries in electric vehicles," *Energy Conversion and Management*, vol. 64, pp. 113–121, 2012.
- [2] J. Meng, G. Luo, M. Ricco, M. Swierczynski, D.-I. Stroe, and R. Teodorescu, "Overview of lithium-ion battery modeling methods for state-of-charge estimation in electrical vehicles," *Applied sciences*, vol. 8, no. 5, p. 659, 2018.
- [3] S. Lee, J. Kim, J. Lee, and B. H. Cho, "State-of-charge and capacity estimation of lithium-ion battery using a new open-circuit voltage versus state-of-charge," *Journal of Power Sources*, vol. 185, no. 2, pp. 1367–1373, 2008.
- [4] J. K. Barillas, J. Li, C. Günther, and M. A. Danzer, "A comparative study and validation of state estimation algorithms for li-ion batteries in battery management systems," *Applied Energy*, vol. 155, pp. 455–462, 2015.
- [5] B. Xia, C. Chen, Y. Tian, W. Sun, Z. Xu, and W. Zheng, "A novel method for state of charge estimation of lithium-ion batteries using a nonlinear observer," *Journal of Power Sources*, vol. 270, pp. 359–366, 2014.
- [6] M. Doyle, T. F. Fuller, and J. Newman, "Modeling of galvanostatic charge and discharge of the lithium/polymer/insertion cell," *Journal of the Electrochemical Society*, vol. 140, no. 6, p. 1526, 1993.
- [7] T. F. Fuller, M. Doyle, and J. Newman, "Simulation and optimization of the dual lithium ion insertion cell," *Journal of the Electrochemical Society*, vol. 141, no. 1, p. 1, 1994.
- [8] D. Di Domenico, A. Stefanopoulou, and G. Fiengo, "Lithium-ion battery state of charge and critical surface charge estimation using an electrochemical model-based extended kalman filter," *Journal of Dynamic Systems, Measurement, and Control*, vol. 132, no. 6, 2010.
- [9] P. G. Blondel, R. Postoyan, S. Raël, S. Benjamin, and P. Desprez, "Observer design for an electrochemical model of lithium ion batteries based on a polytopic approach," *IFAC-PapersOnLine*, vol. 50, no. 1, pp. 8127–8132, 2017.
- [10] P. Blondel, R. Postoyan, S. Raël, S. Benjamin, and P. Desprez, "Nonlinear circle-criterion observer design for an electrochemical battery model," *IEEE Transactions on Control Systems Technology*, vol. 27, no. 2, pp. 889–897, 2018.
- [11] E. Planté, R. Postoyan, S. Raël, Y. Jebroun, S. Benjamin, and D. M. Reyes, "Multiple active material lithium-ion batteries: finite-dimensional modeling and constrained state estimation," *IEEE Transactions on Control Systems Technology*, 2022.
- [12] S. Raël and M. Hinaje, "Using electrical analogy to describe mass and charge transport in lithium-ion batteries," *Journal of Power Sources*, vol. 222, pp. 112–122, 2013.
- [13] P. Bernard, V. Andrieu, and D. Astolfi, "Observer design for continuous-time dynamical systems," *Annual Reviews in Control*, 2022.
- [14] E. Petri, R. Postoyan, D. Astolfi, D. Nešić, and V. Andrieu, "Towards improving the estimation performance of a given nonlinear observer: a multi-observer approach," *IEEE Conference on Decision and Control*, Cancún, Mexico, pp. 583–590, 2022.
- [15] R. Goebel, R. G. Sanfelice, and A. R. Teel, *Hybrid Dynamical Systems: Modeling, Stability, and Robustness*. New Jersey, USA: Princeton University Press, 2012.
- [16] S. J. Moura, F. B. Argomedo, R. Klein, A. Mirtabatabaei, and M. Krstic, "Battery state estimation for a single particle model with electrolyte dynamics," *IEEE Transactions on Control Systems Technology*, vol. 25, no. 2, pp. 453–468, 2016.
- [17] S. Dey, B. Ayalew, and P. Pisu, "Nonlinear robust observers for state-of-charge estimation of lithium-ion cells based on a reduced electrochemical model," *IEEE Transactions on Control Systems Technology*, vol. 23, no. 5, pp. 1935–1942, 2015.
- [18] J. C. Willems, "Deterministic least squares filtering," *Journal of Econometrics*, vol. 118, no. 1-2, pp. 341–373, 2004.
- [19] C. Cai, A. R. Teel, and R. Goebel, "Smooth Lyapunov functions for hybrid systems-part i: Existence is equivalent to robustness," *IEEE Transactions on Automatic Control*, vol. 52, no. 7, pp. 1264–1277, 2007.
- [20] E. D. Sontag, "Input to state stability: Basic concepts and results," in *Nonlinear and Optimal Control Theory*, pp. 163–220, Springer, 2008.
- [21] J. R. Belt, "Battery test manual for plug-in hybrid electric vehicles," tech. rep., Idaho National Lab.(INL), Idaho Falls, ID (USA), 2010.